Mon. Not. R. Astron. Soc. **000**, 1–?? (2001) Printed 11 July 2005 (MN LATEX style file v1.4)

Higher Criticism Statistic: Detecting and Identifying Non-Gaussianity in the WMAP First Year Data

L. Cayón[1], J. Jin[2] and A. Treaster[1]

1. Department of Physics. Purdue University. 525 Northwestern Avenue, West Lafayette, IN 47907-2036.

2. Department of Statistics. Purdue University. 150 N. University Street, West Lafayette, IN 47907-2067.

11 July 2005

ABSTRACT

Higher Criticism is a recently developed statistic for non-Gaussian detection, proposed in Donoho & Jin 2004, where it has been shown to be effective at resolving a very subtle testing problem: whether n normal means are all zero versus the alternative that a small fraction is nonzero. Higher Criticism is also useful in the detection of a non-Gaussian convolution component of cosmic strings in the Cosmic Microwave Background (CMB), see Jin et al. 2004. In this paper, we study how well the anisotropies of the CMB fit with the homogeneous and isotropic Gaussian distribution predicted by the Standard Inflationary model. We find that Higher Criticism is useful for two purposes. First, Higher Criticism has competitive detection power, and non-Gaussianity is detected at the level 99% in the first year WMAP data. We generated 5000 Monte Carlo Gaussian simulations of the CMB maps. By applying the Higher Criticism to all of these maps in wavelet space, we constructed confidence regions of Higher Criticism at levels 68%, 95%, and 99%. We find that the Higher Criticism value of WMAP is outside the 99% confidence region at a wavelet scale of 5 degrees (99.46% of Higher Criticism values based on simulated maps are below the values for WMAP). Second, Higher Criticism offers a way to locate a small portion of data that accounts for the non-Gaussianity. This property is not immediately available for other statistical tests such as the widely-used excess kurtosis test. Using Higher Criticism, we have successfully identified a ring of pixels centered at ($l \approx 209°, b \approx -57°$), which seems to account for the observed detection of non-Gaussianity

at the wavelet scale of 5 degrees. By removing the ring from the WMAP data set, no more prominent deviation from Gaussianity was found. Note that the detection is achieved in wavelet space first. Second, it is always possible that a fraction of pixels within the ring might deviate from Gaussianity even if they do not appear to be above the 99% confidence level in wavelet space. The location of the ring coincides with the cold spot detected in Vielva et al. 2004 and Cruz et al. 2005.

1 INTRODUCTION

The Standard Inflationary model solves the horizon, the flatness, and the monopole problems, and provides a framework for the formation of structure in the universe (Guth 1981, Guth & Pi 1982). Regarding the latter, the Standard Inflationary model predicts the existence of quantum density fluctuations that are amplified during the inflationary period and that grew, through gravitational instabilities, into the galaxies and clusters that populate our universe. These primordial density fluctuations are predicted to form a homogeneous and isotropic Gaussian field. The predicted statistical distribution of the Cosmic Microwave Background (CMB) temperature fluctuations reflects that of the primordial density fluctuations. Testing this prediction has been the aim of many works in the literature. In particular, since the release of the first year of data collected by the WMAP (Wilkinson Microwave Anisotropy Probe) satellite (Bennett et al. 2003), a considerable number of papers have presented different statistical analyses based on data in real space, spherical harmonics, and wavelet space (Park 2004, Eriksen et al. 2004a, Eriksen et al. 2004b, Eriksen et al. 2005, Larson & Wandelt 2004, Hansen et al. 2004, Prunet et al. 2005, Vielva et al. 2004, Cruz et al. 2005, Mukherjee & Wang 2004, Mc.Ewen et al. 2004). All these works have claimed the detection of deviations from the predictions of the Standard Inflationary model in the WMAP data set optimal for CMB studies (see Komatsu et al. 2003). Several other works have presented statistical methods shown to be very powerful in detecting deviations from the Standard Inflationary model in the so-called Internal Linear Combination (ILC) map (Chiang et al. 2003, Coles et al. 2004, Copi et al. 2004, Naselsky et al. 2003, Chiang & Naselsky 2004). In this case the most convincing source of deviations is foreground related.

Deviations from the predictions of the Standard Inflationary model can have a cosmological origin. Non-Gaussianity can be generated under different conditions. A review on the predictions from several alternative scenarios including multi-field inflation, inhomogeneous

reheating, non-linearities in the gravitational potential, and the curvaton-based model can be found in Bartolo et al. 2004. However, these deviations can also be caused by systematic effects or noise associated with the experiment as well as foregrounds (Galactic or extra-galactic). The first year of data collected by the WMAP satellite has undergone careful characterization and examination by the WMAP team in an attempt to fully understand the data set (Page et al. 2003, Hinshaw et al. 2003, Bennett et al. 2003b, Barnes et al. 2003, Jarosik et al. 2003). The detection of deviations indicated in the previous paragraph show the presence of some asymmetry between the northern and southern hemispheres. Moreover, analyses in wavelet space in different regions (north, south, northeast, northwest, southeast, southwest of the Galactic plane) performed by Vielva et al. 2004 and Cruz et al. 2005 indicate that the source of deviations might be a cold spot located at ($l \approx 209^\circ, b \approx -57^\circ$). The nature of the observed deviations is still not clear.

The implementation and development of new statistical methods is indispensable to improve our understanding of the deviations from the Standard Inflationary model predictions, in particular those observed in the WMAP data. There are many kinds of non-Gaussianity, and each type may be sensitive to some statistical tests but immune to others. We need more types of tests, such as Higher Criticism in order to better understand non-Gaussianity. The Higher Criticism (HC) statistic was first proposed in Donoho & Jin (2004) for testing a very subtle problem: given n Gaussian observations with same standard deviations but different means, we want to test whether n means are all zeros versus the alternative that a small fraction of them is nonzero. The fraction of nonzero means is too small to have any effect on the bulk of the observations, so all statistics based on moments (e.g. excess kurtosis (κ)) would generally have no power for detection. With careful calibrations, HC was proved to be optimal in detecting such situations. HC is also competitive for detection in other scenarios. An analysis of simulated CMB on flat patches of the sky using the HC statistics was presented in Jin et al. 2004. The simulated images included CMB signals, as well as cosmic strings and Sunyaev-Zeldovich type emission. Analyses were performed in wavelet and curvelet spaces (Candés & Donoho 2000). The very particular non-Gaussianity introduced by the simulated effects, as well as the restricted size of the sample, resulted in the lower sensitivity of this method in comparison with the traditional κ statistic. However, theoretical studies indicate that the HC statistic will outperform the κ when the sample size gets larger.

Besides its competitive detection power, HC is also valuable in identifying the origin

of detected deviations, offering a way to determine which portion of the data contributes most to the deviation; this property is not available for many other statistics such as κ. As mentioned above, analyses of the WMAP data in wavelet space suggest that the source of the detected deviations is due to the cold temperatures of certain pixels within a spot located in the southern hemisphere. The HC test is especially sensitive to abnormally high amounts of moderately large observations and, as shown in this paper, its application to WMAP data shows deviations from the predictions of the Standard Inflationary model. Moreover, inspection of individual pixel HC values in the WMAP data provides a direct means to identify the pixels at the source of the deviation. No additional region-by-region analysis is needed. The computational cost is therefore strongly reduced, making it a promising test for analyzing future higher resolution data, such as data from the Planck mission*.

The paper is organized as follows. The HC statistical test is described in detail in Section 2. A comparison between the performance of this statistic and that of the kurtosis (κ) and the Maximum (Max) is included in subsection 2.1. The WMAP data is analyzed in real and wavelet spaces. A description of the combination of WMAP data in different channels, the Monte Carlo simulations, and the process followed in wavelet space is included in Section 3. The analysis of the WMAP data is presented in Section 4. Section 5 is dedicated to conclusions and discussion.

2 HIGHER CRITICISM

The HC statistic was first proposed in Donoho & Jin 2004, Jin 2004. Given n independent observations of a distribution which is thought to be slightly deviated from the standard Gaussian, one can compare the fraction of observed significances at a given α-level (i.e. the number of observed values exceeding the upper-α quantile of the standard Gausian) to the expected fraction under the standard Gaussian assumption:

$$\sqrt{n}|(Fraction\ of\ Significance\ at\ \alpha) - \alpha|/(\alpha(1-\alpha))^{0.5}.$$

The HC statistic is then defined as the maximum of the above quantities over all significance levels $0 < \alpha < 1$. Given n individual observations X_i from a distribution which is thought to be symmetric and slightly deviated from the standard Gaussian, there is a simpler equivalent form of HC defined as follows. First, we convert the individual X_i's into individual p-values:

* http://www.rssd.esa.int/index.php?project=PLANCK

$p_i = P\{|N(0,1)| > |X_i|\}$, then we let $p_{(1)} < p_{(2)} < \ldots < p_{(n)}$ denote the p-values sorted in ascending order, define:

$$HC_{n,i} = \sqrt{n}\left|\frac{i/n - p_{(i)}}{\sqrt{p_{(i)}(1-p_{(i)})}}\right|,$$

the HC statistic is then:

$$HC_n^* = \max_i HC_{n,i}$$

or in a modified form:

$$HC_n^+ = \max_{\{i:\, 1/n \leqslant p_{(i)} \leqslant 1-1/n\}} HC_{n,i};$$

we let HC_n refer either to HC_n^* or HC_n^+ whenever there is no confusion. The above definition is slightly different from that in Donoho & Jin 2004, but the ideas are essentially the same.

HC is useful in non-Gaussianity detection when X_i are truly from $N(0,1)$, with the result that $HC_{n,i}$ is approximately distributed as $N(0,1)$ for almost every i. Thus an unusually large HC_n^* or HC_n^+ value strongly implies non-Gaussianity. Moreover, $HC_{n,i}$ also provides *localized* information on deviations from Gaussianity. We can track down the source of non-Gaussianity by studying which portion of the data gives unusually large $HC_{n,i}$.

Previous works have claimed the detection of deviations from the predictions of the Standard Inflationary model in the First Year WMAP data, using the κ statistic in wavelet space (Vielva et al. 2004, Mukherjee & Wang 2004, McEwen et al. 2004). In order to establish a comparison between this statistic and the HC we will include calculations of κ in our analysis as well. For completeness, we will also use the so-called Max statistic. The definitions for these two statistics are provided below. A discussion about the theoretical power of the three statistics to detect deviations from Gaussianity is included in the following subsection.

Kurtosis, κ. For a (symmetric) random variable X, κ is $\kappa(X) = \frac{E[X^4]}{(E[X^2])^2} - 3$, which uses the 4th moment to measure the departure from Gaussianity. κ is useful in non-Gaussianity detection as $\kappa(X_1, X_2, \ldots, X_n) \approx \kappa(X)$ for large n.

Max. The largest (absolute) observation is a classical statistic:

$$M_n = max\{|X_1|, |X_2|, \ldots, |X_n|\}.$$

Max is useful in non-Gaussianity detection because $M_n \approx \sqrt{2\log n}$ when X_i are truly from $N(0,1)$; thus a significant difference between M_n and $\sqrt{2\log n}$ implies non-Gaussianity.

2.1 Comparison of Higher Criticism, Max and Excess Kurtosis

The aim of this section is to establish a simple theoretical comparison between the three statistics applied in this paper. We show the power of the different statistical tests in detecting the distortion generated by a faint non-Gaussian signal (modeled as a function of the decaying rate of the tail of the distribution) superposed on a Gaussian signal. Similar to the analysis presented in Jin et al. 2004, the superposed image can be thought of as $Y = N + G$, where Y is the observed image, N is the non-Gaussian component, and G is the Gaussian component (assumed to have mean zero and dispersion one, $N(0,1)$). We study the power of the three statistics in testing whether $N = 0$ or not.

One can do such a test either in real space (the space of the observations) or, as it is done in this paper, in wavelet space. For sufficiently fine resolution, the wavelet coefficients X_i of Y can be modeled as:

$$X_i = \sqrt{1-\lambda} \cdot z_i + \sqrt{\lambda} \cdot w_i, \qquad 1 \leqslant i \leqslant n,$$

where n is the number of observations, $1 \geqslant \lambda \geqslant 0$ is a parameter, $z_i \overset{iid}{\sim} N(0,1)$ are the transform coefficients of the Gaussian component G, and $w_i \overset{iid}{\sim} W$ are the transform coefficients of the non-Gaussian component N. W is some unknown distribution with vanishing first and third order moment (this constraint is only imposed to simplify the possible range of non-Gaussian distributions, and it will be representative of a Gaussian distribution modified by a few large values contributing to a tail). Without loss of generality, we assume the standard deviation of both z_i and w_i are 1. Phrased in statistical terms, the problem of detecting the existence of a non-Gaussian component is equivalent to discriminating between the null hypothesis and the alternative hypothesis:

$$H_0 : \quad X_i = z_i,$$

$$H_1 : X_i = \sqrt{1-\lambda} \cdot z_i + \sqrt{\lambda} \cdot w_i, \qquad 0 \leqslant \lambda \leqslant 1.$$

$N \equiv 0$ being equivalent to $\lambda \equiv 0$.

In order to obtain a quantitative estimation of the ability of the three statistics to detect the non-Gaussian component, we parametrize the tail probability of W as follows.

$$\lim_{x \to \infty} x^{\alpha} P\{|W| > x\} = C_{\alpha}, \qquad C_{\alpha} \text{ is a constant.}$$

To model increasingly challenging situations as the number of observations increases, we calibrate λ to decay with n as:

$$\lambda = \lambda_n = n^{-r}.$$

To constrain the detectability of such a non-Gaussian distribution superposed to a Gaussian one, we search the r and α parameter space. We define the regions of this space that will be detectable under different statistical tests. It was shown in Jin et al. 2004 that there is a curve in the r-α plane that separates the detectable regions of parameters from the undetectable regions. That curve is given by:

$$r = \begin{cases} 2/\alpha, & \alpha \leqslant 8, \\ 1/4, & \alpha > 8. \end{cases}$$

In Figure 1, we compare the results of HC, Max and κ. When it is possible to detect, HC or Max are better than κ when $\alpha \leqslant 8$. κ is better than HC or Max when $\alpha > 8$.

To conclude this section, we remark that the performance of HC, Max, and κ depends on different situations of non-Gaussianity. Intuitively, Max is designed to capture evidence of unusual behavior of the most extreme observations against the Gaussian assumption. The HC statistic is able to capture unusual behavior of the most extreme observations, as well as unusually large amounts of moderately high observations. Thus HC is better than Max, in general. However, when the evidence against the Gaussian assumption truly lies in the most extreme observations, HC and Max are almost equivalent. In contrast, κ is designed to capture the evidence hidden in the 4th moment. Therefore this statistic depends on the bulk of the data, rather than on a few extreme observations or a small fraction of relatively large observations. Lastly, the HC statistic offers an automatic way to find the area of the data accounting for the non-Gaussianity, while the Max and κ statistics do not have this capability.

3 WMAP FIRST YEAR DATA AND SIMULATIONS

The data collected by the WMAP satellite during the first year of operation is available at the Legacy Archive for Microwave Background Data Analysis (LAMBDA) website[†]. Following Komatsu et al. 2003, the analysis presented in this work is based on a data set obtained by the weighted combination of the released Foreground Cleaned Intensity Maps at bands Q,V and W. Each of these maps can be downloaded in the HEALpix[‡] nested format at resolution $nside = 512$ (total number of pixels being $12 \times nside^2$). The co-added map is obtained by

[†] http://lambda.gsfc.nasa.gov/

[‡] HEALPix http://www.eso.org/science/healpix/

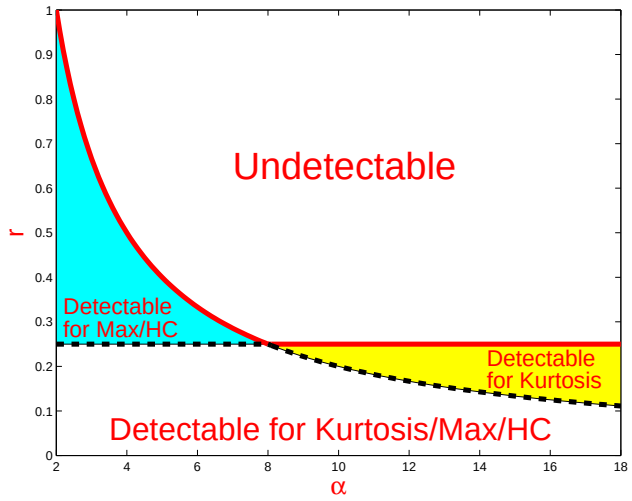

Figure 1. Detectable regions in the $\alpha - r$ plane. With (α, r) in the white region on the top or the undetectable region, all possible statistics fail asymptotically for detection. With (α, r) in the white region on the bottom, both κ and Max/HC are able to detect reliably. While in the blue region to the left, Max/HC is able to detect reliably, but κ completely fails. In the yellow region to the right, κ is able to detect reliably, but Max/HC completely fail asymptotically.

the following combination

$$T(i) = \frac{\sum_{r=3}^{10} T_r(i) w_r(i)}{\sum_{r=3}^{10} w_r(i)}.$$

The temperature at pixel i, $T(i)$ results from the ratio of the weighted sum of temperatures at pixel i at each radiometer divided by the sum of the weights of each radiometer at pixel i. The radiometers Q1, Q2, V1, V2, W1, W2, W3 and W4 are sequentially numbered from 3 to 10. The weights at each pixel, for each radiometer $w_r(i)$, are the ratio of the number of observations $N_r(i)$ divided by the square of the receiver noise dispersion $\sigma_{o,r}$.This results in a co-added map at resolution $nside = 512$. This map is downgraded to resolution $nside = 256$ before the analyses are performed. In order to remove Galactic and point source emission, we applied the most conservative mask provided by the WMAP team, the Kp0 mask. This follows the procedure first presented by Vielva et al. 2004.

In order to detect any possible deviations from the predictions of the Standard Inflationary model we compared the values of several statistics in the WMAP data set described above, with those obtained from 5000 Monte Carlo simulations. The temperature at a certain pixel i (pointing towards a direction characterized by polar angles θ_i and ϕ_i), can be expressed as an expansion in spherical harmonics $Y_{lm}(\theta_i, \phi_i)$

$$T(\theta_i, \phi_i) = \sum_{l,m} a_{lm} Y_{lm}(\theta_i, \phi_i)$$

The Monte Carlo simulations were performed assuming a Gaussian distribution $N(0, C_l)$ for the spherical harmonic coefficients a_{lm} where C_l represents the power spectrum that best

fits the WMAP, CBI and ACBAR CMB data, plus the 2dF and Lyman-alpha data. Beam transfer functions as well as number of observations and receiver noise dispersion were taken into account when simulating data taken by each of the receivers (all of these, as well as the best fit power spectrum are provided by the WMAP team in the LAMBDA website).

The analysis was carried out in both real space and wavelet space. We convolved the WMAP data set and the Monte Carlo simulations with the Spherical Mexican Hat Wavelet (SMHW) at fifteen scales, following the same procedure presented in Vielva et al. 2004 and Cruz et al. 2005. The scales, numbered from 1 to 15, correspond to 13.74, 25.0, 50.0, 75.0, 100.0, 150.0, 200.0, 250.0, 300.0, 400.0, 500.0, 600.0, 750.0, 900.0, and 1050.0 arcmin. In order to avoid border effects caused by the mask included in the WMAP data set and the simulations, analyses are performed outside extended masks defined at each scale. Given a scale, the extended mask is the Kp0 mask plus pixels near the Galactic plane that are within 2.5 times the scale. All of these extended masks were presented in Figure 2 of Vielva et al. 2004. As discussed in the next section, deviations are detected in wavelet space. This shows once again the value of wavelets to provide a space in which certain features that might be causing deviations from the predictions of the Standard Inflationary model are enhanced.

4 ANALYSIS

Based on 5,000 simulations, we calculated the 68%, 95%, and 99% confidence regions for each of the 4 statistics (κ, Max, and the two HC tests) at each of the 15 wavelet scales used. We used two-sided confidence regions for κ, as it is symmetric about 0 under the null hypothesis that the data is Gaussian. Max and HC statistics are defined so that the larger the statistic, the stronger the evidence against the null hypothesis. Therefore, we used one-sided confidence regions for these statistics.

Figure 2 shows the results obtained based on κ. Dots denote the value of this statistic for the WMAP data set. Bands outlined by dashed, dotted-dashed, and solid lines correspond to the 68%, 95%, and 99% confidence regions respectively (symbols and lines will represent the same in the figures included in this paper unless a comment is added). Clearly, the results agree with those presented in Vielva et al. 2004. Figures 3 and 4 show the new results based on the Max and HC statistical tests. The WMAP data appears outside the 99% confidence level obtained based on the predictions of the Standard Inflationary model at scale 9 (300 arcmin) for these three tests. In particular, $\approx$ 99.46% of the 5000 simulations have Max

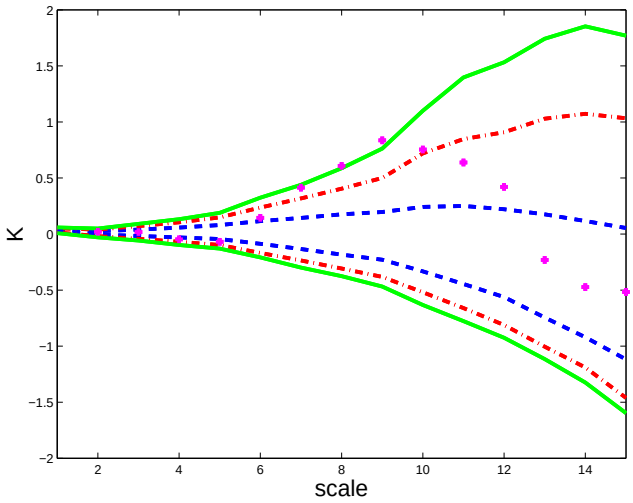

Figure 2. Values of the κ statistic for the analyzed WMAP data set (dots). The bands outlined by dashed, dotted-dashed and solid lines correspond to the 68%, 95% and 99% confidence regions respectively.

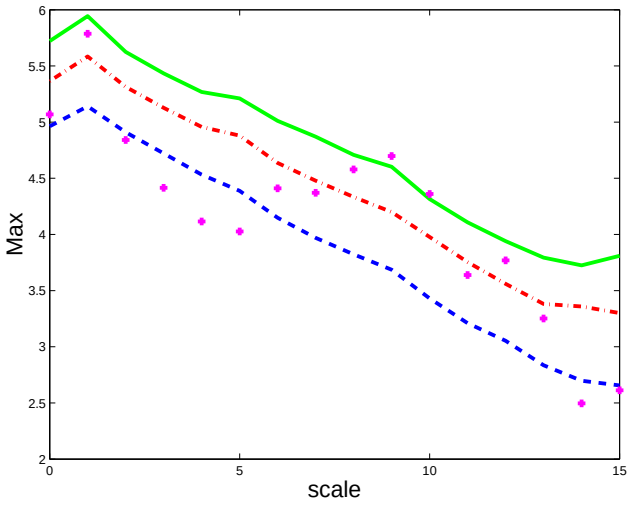

Figure 3. Values of the Max statistical test for the analyzed WMAP data set (dots). The dashed, dotted-dashed and solid lines correspond to the 68%, 95% and 99% confidence levels respectively.

and HC/HC^{+} values below the one obtained from the WMAP data set. Therefore in this particular case these statistics are as competitive as the kurtosis in detecting deviations from the assumed null hypothesis.

4.1 Location of the outlying pixels provided by the Higher Criticism statistic

As discussed above, the HC statistical tests introduced in this paper are able to detect deviations from the Standard Inflationary model in the WMAP data at scales around 300 arcmin. Moreover, the power of this new test resides in providing a direct way to determine which pixels in the WMAP data set are generating these deviations. By comparing the values of the HC test at each pixel, with the value that defines the 99% confidence limit at

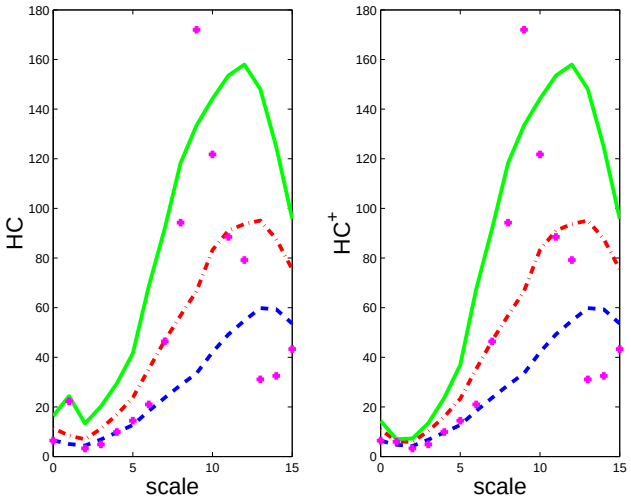

Figure 4. Values of the HC/HC^{+} statistical tests for the analyzed WMAP data set (dots). The dashed, dotted-dashed and solid lines correspond to the 68%, 95% and 99% confidence levels respectively.

scale 9, we were able to extract a total of 490 pixels that are causing the detected deviation. Figure 5 shows the individual pixel values of the HC statistic for the WMAP data set at scale 9. The selected pixels above the 99% limit are plotted in the map shown in Figure 6. As can be seen, these pixels define a ring centered at position ($l \approx 209°, b \approx -57°$). It is important to note that the correlations introduced by the convolution with the wavelet need to be taken into account in order to properly interpret this result. Some pixels within the ring could also initially (in the map in real space) deviate from Gaussianity.

4.2 Effects of the subtraction of pixels at the source of the detection

Removal of the pixels in the ring from the analysed WMAP data resulted in a set of data compatible with the predictions from the Standard Inflationary model (see Figure 7). The deviation observed in the κ statistic at the wavelet scale of 5 degrees, in this paper as well as in previous papers by Vielva et al. 2004, Cruz et al. 2005, Mukherjee & Wang 2004, McEwen et al. 2004, disappeared as the pixels in the ring ($l \approx 209°, b \approx -57°$) were removed. These pixels are part of the cold spot pointed out by Vielva et al. 2004 and Cruz et al. 2005 as being the source of the observed deviations. The Max and the HC values decrease as well (after removal of the pixels in the ring) fitting now within the 68% confidence region. The Higher Criticism statistic is useful by offering an automatic detection of the non-Gaussian portions of the data. This characteristic is not easily available for other tests, such as Kurtosis.

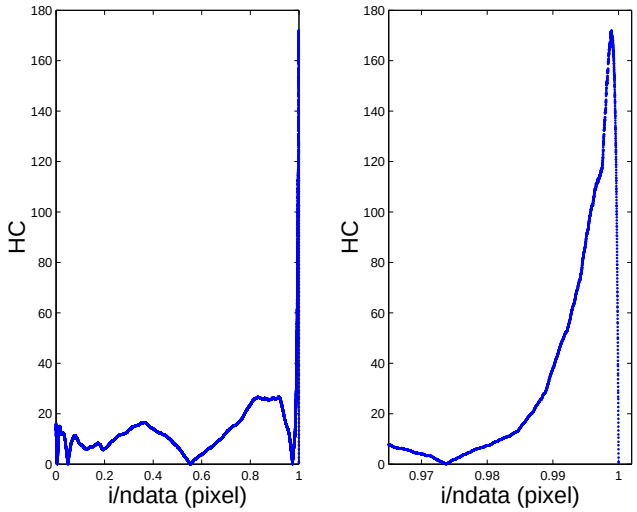

Figure 5. Values of the HC statistical test at every pixel of the analyzed WMAP data set. After sorting all the p-values, a number is assigned to each pixel i. That number goes from 0 (pixel with the smallest p-value) to the number of data (pixel with the largest p-value). The HC values at each pixel are plotted against $i/number\ of\ data$. The region corresponding to the extreme values of HC is shown in the figure on the right panel.

Figure 6. A quarter of the whole sky showing the location of the WMAP pixels with HC values above the extreme of the 99% limit obtained from 5000 simulations.

5 CONCLUSIONS AND DISCUSSION

This paper presents an analysis of the compatibility of the distribution of the CMB temperature fluctuations observed by WMAP with the predictions from Standard Inflation. The analysis is based on the recently developed HC statistic. This statistic is especially sensitive to two types of deviations from Gaussianity: an unusually large amount of moderately significant values or a small fraction of unusually extreme values. In both of these cases the HC statistic is optimal (Donoho & Jin 2004, Jin et al. 2004). Moreover, the definition of the statistic naturally suggests a direct way to locate the possible sources of non-Gaussianity. Even if the wavelet transform is a linear process, the original distribution is slightly distorted as the scale of the wavelet, and the area covered by the mask, increase. We are working on

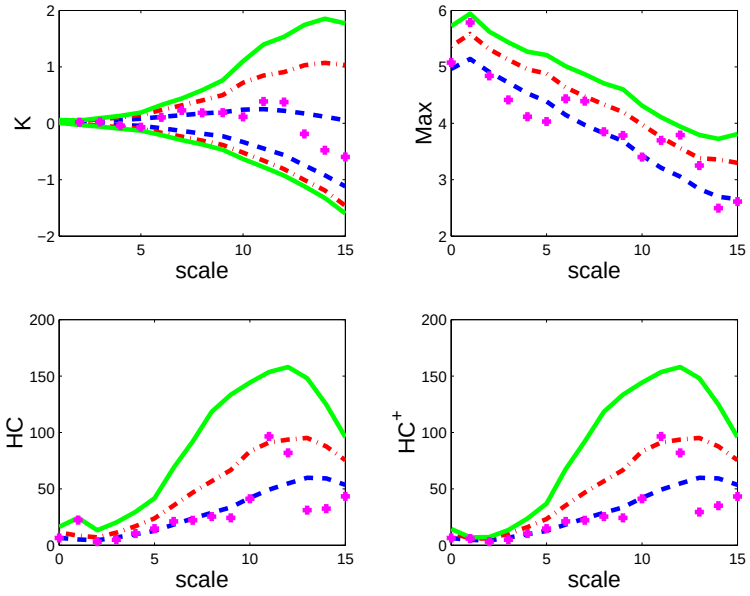

Figure 7. Values of κ, Max and HC tests for the analyzed WMAP data set after subtracting the pixels that were causing the deviations from the predictions of the Standard Inflationary model (dots). The bands outlined by dashed, dotted-dashed and solid lines correspond to the 68%, 95% and 99% confidence regions respectively for κ. The dashed, dotted-dashed and solid lines correspond to the 68%, 95% and 99% confidence levels respectively for Max, HC and HC^+.

improving the power of the HC statistic to be optimal in the detection of deviations from Gaussianity when applied in wavelet space.

We compared the performance of the HC statistic with that of κ and Max. The comparison was based on the analysis of the first year WMAP data, in real space and in wavelet space. Distributions of the three statistics were built on 5000 simulations assuming the Standard Inflationary model predictions as well as the constraints coming from the WMAP observations. The three statistics provided comparable results, pointing to the presence of deviations at a wavelet scale of 5 degrees. We made use of the HC statistic to automatically identify the pixels in the WMAP data set that were causing such deviations. A ring centered at $(l \approx 209^\circ, b \approx -57^\circ)$ containing 490 pixels was shown to be the cause behind the detected deviations. Removal of this set of pixels from the WMAP data made the data compatible with the predictions from the Standard Inflationary model. One should be cautious when interpreting this result. The detection is achieved in wavelet space. Even if only the pixels in the ring appear as outliers of the HC distribution at wavelet scale of 5 degrees, some other pixels whithin the ring could be involved in the observed deviation. Convolution with the wavelet introduces correlations between pixels that need to be properly taken into account in the definition of the statistic to allow a correct interpretation. It is important to note that the pixels selected as the source of the observed deviations are part of the cold spot pointed out by Vielva et al. 2004 and Cruz et al. 2005. A careful study of the possible influence of

foregrounds, noise, and beam distortion and assumption of a certain power spectrum was carried out in those two papers.

To conclude we would like to remark on the power of the HC statistic for detecting and locating possible sources of non-Gaussianity. In particular, regarding analysis of the CMB, the HC statistic can be useful at several steps in the data processing and final analysis, from the study of distortions caused by systematic effects in the time-ordered data to the study of compatibility of the statistical distribution of the observed temperature fluctuations with predictions from theories of the very early universe.

ACKNOWLEDGEMENTS

We thank P. Vielva for providing the extended masks used at different wavelet scales. We would like to thank Douglas Crabill for helping with some of the figures. We acknowledge the use of the Legacy Archive for Microwave Background Data Analysis (LAMBDA). Support for LAMBDA is provided by the NASA Office of Space Science. Some of the results in this paper have been derived using the HEALPix (Górski, Hivon, and Wandelt 1999) package. L.C. and A.T. acknowledge the Indiana Space Grant Consortium for financial support. A.T. acknowledges the Spira Fellowship (Summer 2004 and Summer 2005).

REFERENCES

Barnes, C. et.al., 2003, ApJS, 148, 51

Bartolo, N., Komatsu, E., Materrese, S. & Riotto, A. 2004, Phys. Rept. 402, 103

Bennett, C.L. et al. 2003, ApJS, 148, 1

Bennett, C.L. et.al., 2003b, ApJS, 148, 97

Candés, E.J. & Donoho, D.L. 2000, In *Curve and Surface Fitting: Saint-Malo 1999*, Nashville, TN. Editors: Cohen, A., Rabut, C. & Schumaker, L.L.. Vanderbilt University Press, pag. 105

Chiang, L.-Y., Naselsky, P.D., Verkhodanov, O.V. & Way, M.J. 2003, ApJ, 590, L65

Chiang, L.Y. & Naselsky, P.D. 2004, astro-ph/0407395

Coles, P., Dineen, P., Earl, J. & Wright, D. 2004, MNRAS, 350, 989

Copi, C.J., Huterer, D. & Starkman, G.D. 2004, Phys.Rev.D, 70, 043515

Cruz, M., Martínez-González, E., Vielva, P. & Cayón, L. 2005, 356, 29

Donoho, D. & Jin, J. 2004, *Ann. Statist.*, **32**, 962

Eriksen, H.K., Novikov, D.I., Lilje, P.B., Banday, A.J. & Górski, K.M. 2004a, ApJ, 612, 64

Eriksen, H.K., Hansen, F.K., Banday, A.J., Górski, K.M. & Lilje, P.B. 2004b, ApJ, 605, 14

Eriksen, H.K., Banday, A.J., Górski, K.M. & Lilje, P.B. 2005, ApJ, 622, 58

Górski, K.M., Hivon, E. & Wandelt, B.D. 1999, in Proceedings of the MPA/ESO Cosmology Conference "Evolution of Large-Scale Structure", eds. A.J. Banday, R.S. Sheth and L. Da Costa, PrintPartners Ipskamp, NL, pp. 37-42 (also astro-ph/9812350)

Guth, A.H. 1981, Phys.Rev.D., 23, 347

Guth, A.H. & Pi, S.-Y. 1982, Phys.Rev.Lett., 49, 1110

Hansen, F.K., Banday, A.J. & Górski, K.M. 2004, astro-ph/0404206

Hinshaw, G. et.al., 2003, ApJS, 148, 63

Jarosik, N. et.al., 2003, ApJS, 148, 29

Jin, J. 2004, Institue of Mathematical Statistics Monograph, No. 45, 255

Jin, J., Starck, J.-L., Donoho, D.L., Aghanim, N. & Forni, O. 2004, submitted to EURASIP Journal on Applied Signal Processing, special issue on "Applications of Signal Processing in Astrophysics and Cosmology"

Komatsu, E. et al. 2003, ApJS, 148, 119

Larson, D.L. & Wandelt, B.D. 2004, ApJ, 613, L85

McEwen, J.D., Hobson, M.P., Lasenby, A.N. & Mortlock, D.J. 2005, MNRAS, 359, 1583

Mukherjee, P. & Wang, Y. 2004, ApJ, 613, 51

Naselsky, P.D., Doroshkevich, A.G. & Verkhodanov, O.V. 2003, ApJ, 599, L53

Page, L. et al. 2003, ApJS, 148, 39

Park, C.-G. 2004, MNRAS, 349, 313

Prunet, S., Uzan, J.-P., Bernardeau, F. & Brunier, T. 2005, Phys. Rev. D, 71, 083508

Vielva, P., Martínez-González, E., Barreiro, R.B., Sanz, J.L. & Cayón, L. 2004, ApJ, 609, 22